Supplementary Information - Selectively accessing the hotspots of optical nanoantennas by self-aligned dry laser ablation

Christian Schäfer,[a] Pradeep N. Perera,[b,c] Florian Laible,[a] Deirdre L. Olynick,[b,d] Adam M. Schwartzberg,[b] Alexander Weber-Bargioni,[b] Stefano Cabrini,[b] Peter J. Schuck,[b,e] Dieter P. Kern[a] and Monika Fleischer*[a]

[a] *Institute for Applied Physics and Center LISA⁺, Eberhard Karls Universität Tübingen, Auf der Morgenstelle 10, 72076 Tübingen, Germany. * E-Mail: monika.fleischer@uni-tuebingen.de*

[b] *The Molecular Foundry, Lawrence Berkeley National Laboratory, 1 Cyclotron Road, Building 67, Berkeley, CA94720, USA.*

[c] *Present address: Gemological Institute of America, New York, NY 10036, USA.*

[d] *Present address: UCSF Helen Diller Family Comprehensive Center, San Francisco, CA 94158, USA.*

[e] *Present address: Department of Mechanical Engineering, Columbia University, New York, New York 10027, USA.*

Optical images of grids of spots in which laser ablation occurred with different spacing

To better illustrate the connection between the scanning electron microscopy and fluorescence images in Fig. 5, corresponding overview images taken in an optical microscope are shown in Fig. S1 below. The orange squares each correspond to a 25 x 25 µm^2 array of densely patterned gold nanocones. The nanocones are too small and too closely spaced to be resolved by optical microscopy. The brighter edges around the squares correspond to the unpatterned substrate. The samples are covered by MAC resist. The mapping mode of the scanning stage was used to ablate the MAC in a grid with a centre-to-centre distance of few µm on each array of cones.
In Fig. S1a), a top-view of a grid of areas in which laser ablation occurred (bright spots) with a spacing of ~ 2 µm can be seen within the patterned square, in analogy to the ablated areas in Fig. 5a) and 5b). The brighter colour stems from the cone tips being exposed within the resist matrix, plus from a potentially reduced resist thickness in the laser focus. One can see that the elliptical shapes viewed under 60° in Fig. 5a) correspond to roughly circular areas when viewed from the top. It can also be discerned that the exposure time was increased from the right to the left, leading to increasing ablation around the cones (brighter spots). In Fig. S1b) a grid of areas with laser ablation with a spacing of ~ 4 µm is shown within the patterned square. This larger spacing was further employed for BSA tests as in Fig. 5c) for better distinction between the different areas. After depositing the BSA on the sample, a lift-off in acetone was applied such that BSA only remained in areas where the MAC resist had been removed. After the lift-off process the intensity from the BSA molecules was recorded in fluorescence images, which show that the BSA signal originates from the regions in which laser ablation occurred.

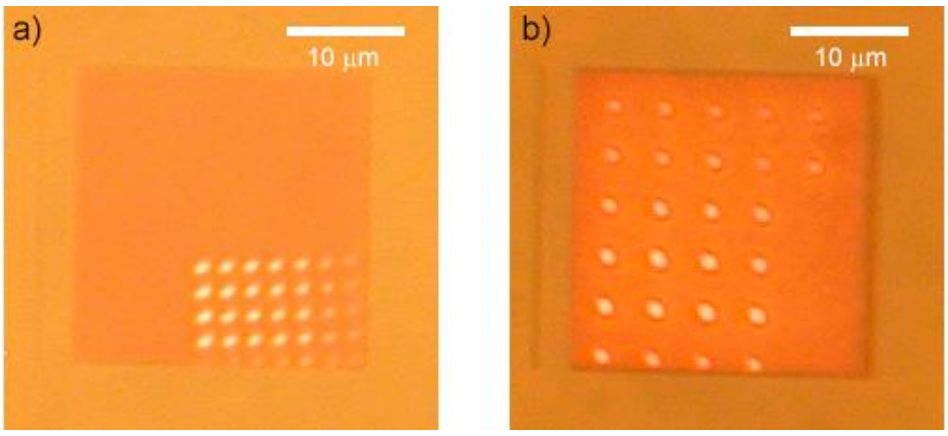

Figure S1: Sample optical microscopy images of two 25 x 25 µm^2 arrays of densely patterned nanocones (orange squares) covered by MAC resist. The areas where ablation occurred appear as bright spots. a) 7 x 5 grid of laser ablated areas with a centre-to-centre spacing of 2 µm, as in Fig. 5a) and 5b). The exposure time was increased from the right to the left. b) 5 x 6 grid of laser ablated areas with a centre-to-centre spacing of 4 µm. The larger spacing was employed for BSA tests as in Fig. 5c) for better distinction between the different areas. The BSA spots seen in fluorescence microscopy are localized at grid positions where ablation occurred.

Near-field distributions around gold nanocones under different illumination angles

To demonstrate the near-field distribution around nanocones, COMSOL Multiphysics simulations were performed for three different configurations of a gold nanocone (base diameter and height of 100 nm) situated on an indium tin oxide (ITO) substrate: Fig. S2 (left column) shows the cone embedded in 4-methylacetoxy-calix[6,8]arene (MAC) resist (refractive index ~1.6) up to 20 nm above the tip; Fig. S2 (middle column) shows the cone embedded in MAC with the resist being removed from the tip (simplified as a planar resist layer up to 20 nm below the tip); and in Fig. S2 (right column), the cone in air is seen after MAC removal. Depending on the polarization of the electric field components of the incoming light, electric near-fields are predominantly excited either near the cone tip or near the base edge. Fig. S2 shows the three cases of a planar wave incident at 85° (top row) where strong near-fields are observed near the apex, a planar wave at 30° incidence corresponding to the limiting angle of an objective with NA = 0.5 (middle row), and a planar wave at perpendicular incidence, leading exclusively to near-fields at the cone base.

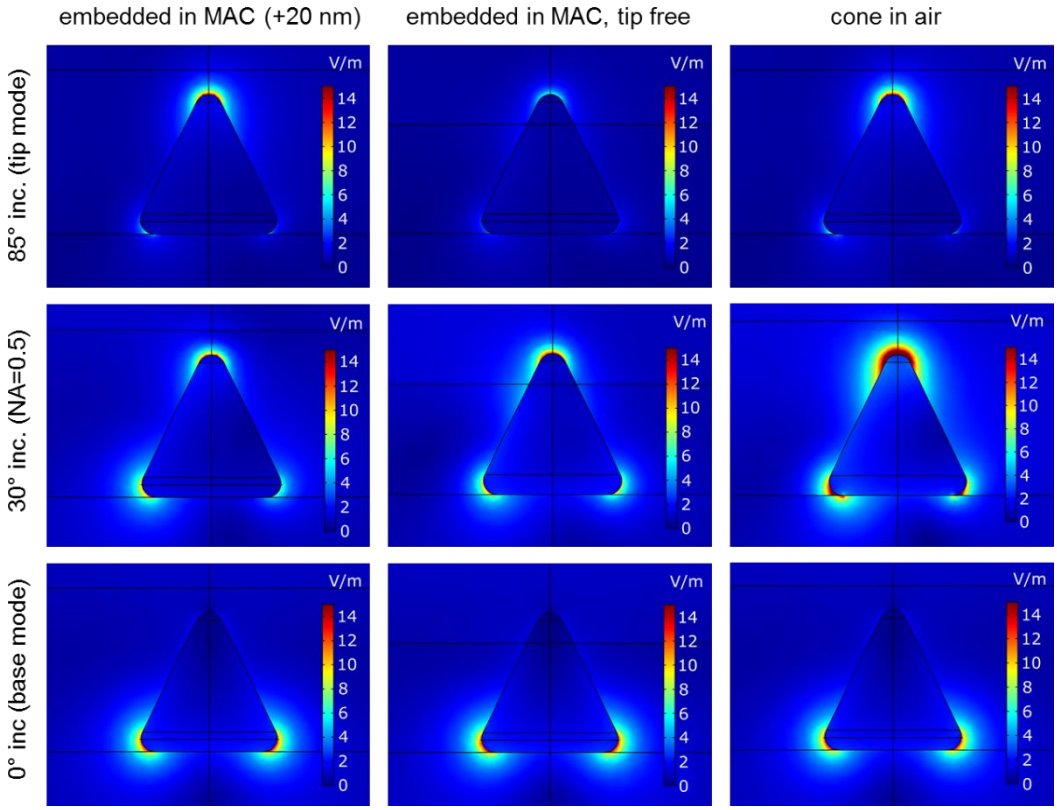

Figure S2: COMSOL Multiphysics finite element method simulations of the near-field distributions around a gold nanocone excited in different configurations at the respective resonance wavelength. Plotted is the electric field norm on a colour scale of 0 to 15 V/m for an incident field of 1 V/m. Substrate: ITO, cone height and cone base diameter: 100 nm, embedding media: MAC resist (refractive index ≈ 1.6) and/or air (n ≈ 1.0).
Left column: cone fully embedded in MAC resist (up to 20 nm above the tip); middle column: cone after tip ablation (resist removed up to 20 nm below the tip); right column: cone in air after resist removal.
Top row: Illumination with a plane wave under an angle of 85° relative to the perpendicular: Excitation of the near-field at the cone tip. Middle row: Illumination with a plane wave under an angle of 30° (from top left), corresponding to the limiting angle for a numerical aperture NA = 0.5: Excitation of near-fields at the cone tip and base edge (plotted at the resonance wavelength of the tip mode). Bottom row: Illumination with a plane wave under perpendicular incidence: Excitation of the near-field at the cone base.